

High precision determination of the elastic strain of InGaN/GaN multiple quantum wells

M. F. Wu,^{a)} Shengqiang Zhou, and Shude Yao

Department of Technical Physics, Peking University, Beijing 100871, People's Republic of China
and Instituut voor Kern-en Stralingsfysika, University of Leuven, B-3001 Leuven, Belgium

Qiang Zhao and A. Vantomme

Instituut voor Kern-en Stralingsfysika, University of Leuven, B-3001 Leuven, Belgium

B. Van Daele, E. Piscopiello, and G. Van Tendeloo

Electron Microscopy for Materials Research (EMAT), University of Antwerp, Belgium

Y. Z. Tong, Z. J. Yang, T. J. Yu, and G. Y. Zhang

School of Physics, State Key Laboratory for Mesoscopic Physics, Peking University, Beijing 100871,
People's Republic of China

(Received 27 May 2003; accepted 1 March 2004; published 16 April 2004)

The composition, elastic strain, and structural defects of an InGaN/GaN multiple quantum well (MQW) are investigated using a combination of x-ray diffraction, transmission electron microscopy, and Rutherford backscattering/channeling. None of the applied techniques alone can unambiguously resolve the thickness of the individual layers, the In composition in the wells, and the elastic strain. These three parameters directly determine the optical properties of the MQW. It is shown that only a combination of these measurements reveals the full structural characterization of the nitride multilayer. A clear correlation between the defect density of In distribution and strain relaxation is evidenced. The experimental result of the ratio of the average perpendicular elastic strain $\langle e^\perp \rangle$ and the average parallel elastic strain $\langle e^\parallel \rangle$, $\langle e^\perp \rangle / \langle e^\parallel \rangle = -0.52$, is in excellent agreement with the value deduced from the elastic constants. © 2004 American Vacuum Society.

[DOI: 10.1116/1.1715085]

I. INTRODUCTION

InGaN/GaN multiple quantum wells (MQWs) are currently used as the active layer for most light-emitting diodes and laser diodes devices. The designed structure and the composition of the MQWs are normally set by the growth conditions. Subsequently, determining the exact structure and its composition are crucial to optimizing the growth procedure and the properties of the MQWs. Most frequently, the indium composition in InGaN layers is determined by x-ray diffraction (XRD). This may lead to a strong overestimation of the In content in the case where the epilayer is strained.¹⁻⁵ However, Rutherford backscattering spectrometry (RBS) is a powerful technique to study the composition of layered structures. In particular, it is possible to determine the In content x in $\text{In}_x\text{Ga}_{1-x}\text{N}$ accurately (with an accuracy of ± 0.005)^{1,2} with RBS. However, due to the limited depth resolution (approximately 3–10 nm, depending on the experimental conditions), RBS alone does not allow us to determine the In concentration in the very thin InGaN layers in a MQW, if both the thickness t_w and t_b of the InGaN layer and GaN layer in the MQW, respectively, are unknown. Nevertheless, the angular separation of the satellite peaks in the XRD pattern and transmission electron microscopy (TEM) (for both real space images and reciprocal space diffraction patterns) can be used to determine the t_w and t_b values. Consequently, RBS combined with XRD and TEM is a reliable

way to unambiguously study the exact In content in MQWs and to subsequently determine the elastic strain of the MQW. Both parameters, the In concentration and the strain, are crucial. The In concentration directly determines the band gap, hence, the wavelength of the emitted light. While the strain will induce a piezoelectric field in GaN-based systems, thus indirectly influencing the effective band gap.^{3,6} The strain of single InGaN or AlGaIn layers can be determined by a combination of RBS and XRD.^{5,7} However, so far no strain data of MQWs have been reported. It should be stressed that unlike the situation of a single InGaN or AlGaIn layer, the XRD peaks of a periodical multilayer exhibit a satellite pattern. The strain derived from this pattern is an average value corresponding to the average composition of the MQWs. From the XRD data published in literature, limited information on the strain in MQWs can be deduced. For a $[7.6 \text{ nm In}_{0.17}\text{Ga}_{0.83}\text{N}/10.4 \text{ nm GaN}]_{5x}$ MQW, an average perpendicular elastic strain value of $\langle e^\perp \rangle \approx 0.4\%$ can be estimated from the x-ray $\theta-2\theta$ scans in Fig. 1 in Ref. 8. However, Korakakis *et al.*⁹ have determined average lattice constants $\langle a_{\text{epi}} \rangle = 0.3154 \text{ nm}$, $\langle c_{\text{epi}} \rangle = 0.5185 \text{ nm}$ for a $[5 \text{ nm Al}_{0.2}\text{Ga}_{0.8}\text{N}/5 \text{ nm GaN}]_{15x}$ MQW. Hence, an average perpendicular elastic strain $\langle e^\perp \rangle = 0.40\%$ and an average parallel elastic strain $\langle e^\parallel \rangle = -0.85\%$ can be deduced. In this work, we illustrate how the structure, the In composition, and the crystalline quality of the InGaN/GaN MQW can be determined with a combination of XRD, TEM, and RBS/channeling. Subsequently, we present a quantitative analysis of the average strain of the MQW using XRD.

^{a)}Electronic mail: mingfang@public.fhnet.cn.net

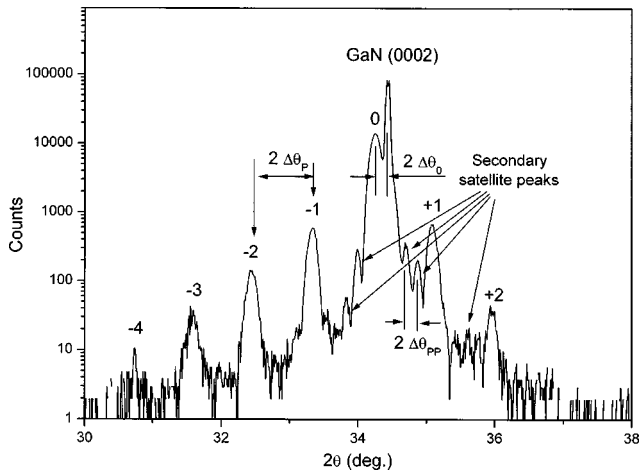


FIG. 1. X-ray θ - 2θ scan of the (0002) diffraction from the InGaN/GaN MQW sample.

II. EXPERIMENT

The sample used in this research was grown on an $\text{Al}_2\text{O}_3(0001)$ substrate by an AXT 2000HT metal-organic chemical vapor deposition system at low pressure (0.1 atm). High-purity H_2 and N_2 were used as carrier gases. First, the substrate was heated to 1200°C under flowing H_2 for 10 min. Subsequently, the temperature was decreased to 540°C for growing a 25 nm GaN nucleation layer. After this, a $1.0\ \mu\text{m}$ undoped GaN layer and $2.5\ \mu\text{m}$ GaN layer doped with Si at a concentration of $5 \times 10^{18}/\text{cm}^3$ were grown consecutively at 1180°C using H_2 as a carrier gas. Finally, five periods of InGaN/GaN were grown at 790°C using N_2 as a carrier gas. Trimethylgallium, trimethylindium, ammonia, and silane (10 ppm in H_2) were used as Ga, In, N, and Si sources, respectively. The typical growth rate is about 2000 nm/h. The composition and the thickness of the different layers were controlled by the flow of precursors and the time of growth. The nominal structure of the sample was $[7.3\ \text{nm GaN}/3.0\ \text{nm In}_{0.2}\text{Ga}_{0.8}\text{N}]_{5x}/3.5\ \mu\text{m GaN}/\text{Al}_2\text{O}_3(0001)$.

Synchrotron radiation ($\lambda=0.154\ \text{nm}$) produced by the Beijing Synchrotron Radiation Facility (BSRF) was used to perform x-ray θ - 2θ scans of the (0002) and (10 $\bar{1}4$) diffractions from the sample. A JEOL 4000EX high-resolution transmission electron microscope was used to study the MQW microstructure using conventional diffraction contrast imaging and high-resolution imaging. A 2 MeV He^+ beam produced by a 5SDH-2 Pelletron was used for RBS/channeling measurements. The sample was mounted on a high-precision ($\pm 0.01^\circ$) three-axis goniometer for precise control of the orientation of the sample relative to the He^+ beam.

III. RESULTS AND DISCUSSION

A. X-ray θ - 2θ diffraction from the (0002) planes

Figure 1 shows the x-ray θ - 2θ scans of the (0002) diffraction from the MQW sample. In addition to the strongest

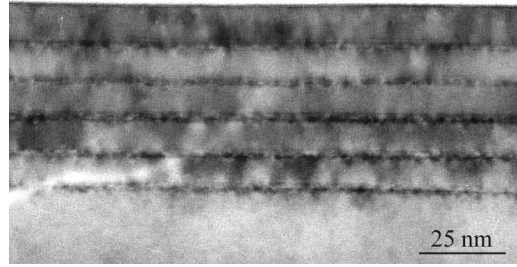


FIG. 2. Cross-sectional TEM image, taken in a (0002) two-beam diffraction condition, showing the five periods of the InGaN/GaN MQW.

GaN(0002) diffraction peak from the thick buffer GaN layer, the satellite peaks from the MQW are displayed up to the fourth order. The $\Delta\theta_P$ determined from the angle between the satellite peaks is 0.44° , hence, the MQW period (the sum of well and barrier thickness) $L=t_w+t_b=\lambda/(2\Delta\theta_P \cdot \cos\theta_B)=10.5\ \text{nm}$. Here, $\theta_B=17.278^\circ$ is the Bragg angle of the GaN(0002) diffraction. In the diffraction pattern, the secondary satellite peaks are also visible. The angular spacing of these secondary satellites is $2\Delta\theta_{PP}$, from which the total thickness of MQW is calculated: $NL=\lambda/(2\Delta\theta_{PP} \cdot \cos\theta_B)=51.5\ \text{nm}$.¹⁰ Knowing that $N=5$, one deduces $L=10.3\ \text{nm}$, confirming the result obtained from $\Delta\theta_P$. The average perpendicular strain of the MQW can be determined from the angular spacing $2\Delta\theta_0$ between the zero-order peak of the MQW and the GaN(0002) peak, as will be discussed below.

B. Microstructural analysis

The cross-sectional TEM image in Fig. 2 shows the five periods of the MQW. Thicknesses t_b of the GaN barrier and t_w of the InGaN quantum wells are, respectively, $8.0 \pm 0.5\ \text{nm}$ and $2\text{--}3\ \text{nm}$. These values are in agreement with the designed structure. The relatively large errors of t_b and t_w are a result of the poorly defined interfaces. The TEM results are also consistent with the values of $L=10.5\ \text{nm}$ and $NL=51.5\ \text{nm}$ deduced from the $\Delta\theta_P$ and $\Delta\theta_{PP}$ values in Fig. 1. Although these values are shown in poor contrast in Fig. 2, a high density of growth defects is present in the InGaN quantum-well region. These defects can be defined as an insertion or extraction of (0002) planes. The extraction or insertion of (0002) planes is only found in the InGaN quantum wells, while the stacking disorder is present in the entire quantum-well-barrier structure. A high-resolution TEM image, taken along the $[11\bar{2}0]$ zone axis, is shown in Fig. 3(a). The bright dots in Fig. 3(a) correspond to the Ga columns in the lattice. In high-resolution TEM images, the defects can be clearly seen. The arrow in Fig. 3(a) indicates the position of an extra (0002) plane, while the brackets indicate a stacking disorder (an A-B stacking sequence next to an A-C stacking sequence). Similar to the satellite peaks observed by XRD, electron diffraction [Fig. 3(b)] also exhibits satellite peaks (see inset) next to the (0002) reflection. This indicates an almost perfect InGaN-GaN sequence.

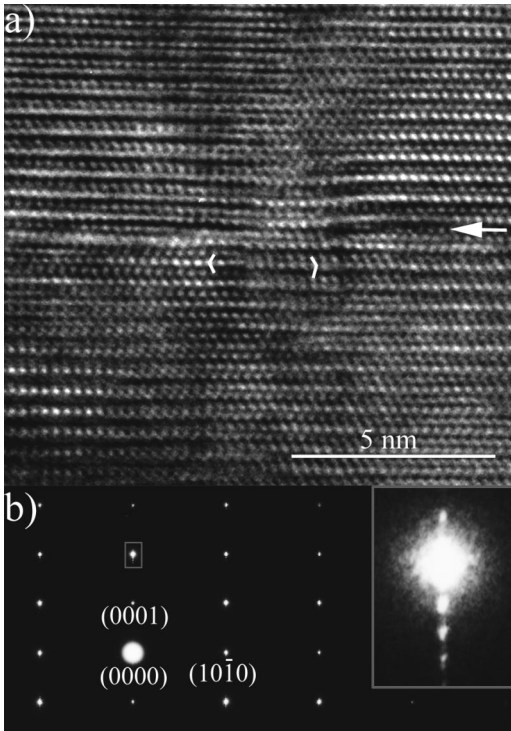


FIG. 3. (a) High-resolution image ($[1\bar{1}20]$ orientation) of an InGaN quantum well showing the most common defects. The arrow indicates an extra (0002) plane; the brackets indicate a stacking disorder. (b) Corresponding selected area diffraction pattern. The inset is an enlargement of the (0002) reflection showing a satellite pattern similar to the XRD pattern of Fig. 1.

C. Simulation of the x-ray diffraction patterns

In order to get more detailed information about the structure of the MQW, a simulation is made to fit the experimental XRD data (Fig. 4). From this procedure, $t_b = 7.7$ nm and $t_w = 2.7$ nm with an error of ± 0.1 nm are obtained. Furthermore, this simulation also determines the In content x to be 0.13 in the $\text{In}_x\text{Ga}_{1-x}\text{N}$ layers. However, one should be aware that this result is obtained based on the assumption that the

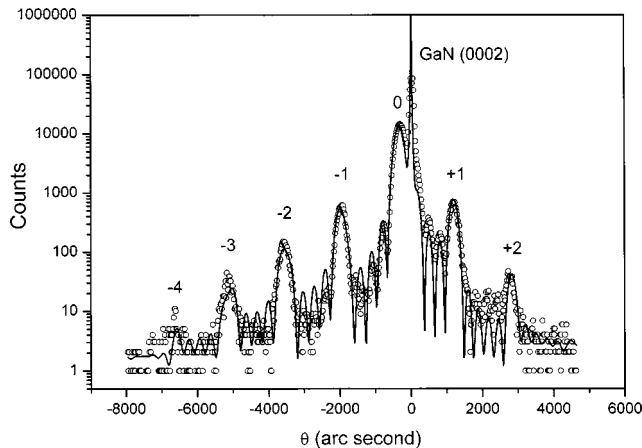


FIG. 4. Fitting of the (0002) diffraction data by the simulation. t_w , t_b , and x values are obtained from the simulation.

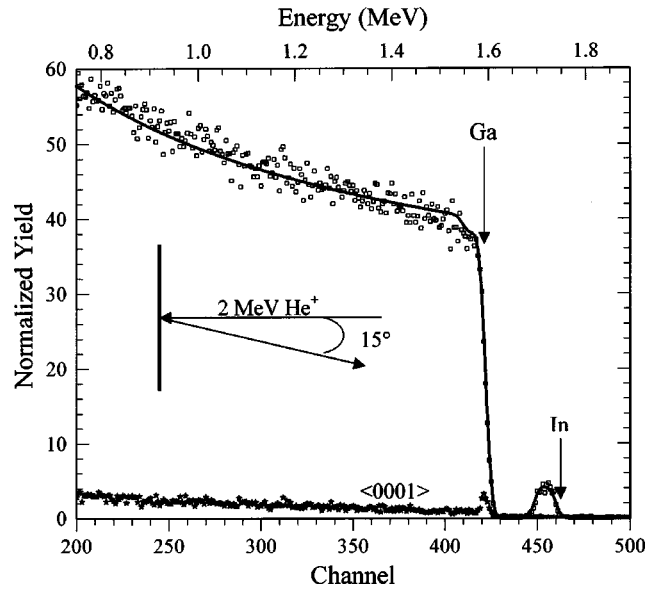


FIG. 5. Random (\square), $\langle 0001 \rangle$ axis aligned (\star), and simulated (solid line) RBS spectra of the InGaN/GaN MQW sample. From the simulation, an x value of 0.16 is obtained.

epilayer is fully strained, resulting in an underestimation of the x value in the case where the epilayer is partially relaxed.

D. Determination of the In content

Figure 5 shows the random and aligned RBS spectra of the sample. The geometry used in the backscattering measurements is shown in the inset. The arrows labeled Ga and In indicate the energy for backscattering from Ga and In atoms at the surface. The small In peak corresponds to the backscattering from the In atoms in the MQW. Using the t_w and t_b values from the simulation of the XRD data, a simulation (solid line in Fig. 5) of the random spectrum given by the RUMP program¹¹ indicates that the composition and the structure of this sample is $[7.7 \text{ nm GaN}/2.7 \text{ nm In}_{0.16}\text{Ga}_{0.84}\text{N}]_{5x}/\text{GaN}$. The In content in the $\text{In}_x\text{Ga}_{1-x}\text{N}$ layer determined by RBS, $x = 0.16$, is independent of the strain in the multilayer. This value indicates that $x = 0.13$, as obtained from the simulation of XRD data, is certainly underestimated and that the epilayer is, in fact, not fully strained, but partially relaxed. Such an accurate determination of the x value is crucial for the subsequent determination of the elastic strain. From the $\langle 0001 \rangle$ aligned spectrum, a minimum yield $\chi_{\text{min}} = 2.4\%$ is obtained for both the In and Ga signal, indicating the excellent crystalline quality of the MQW.

E. Calculation of the average perpendicular elastic strain

In Fig. 1, the position of the zeroth peak relative to the GaN(0002) peak (i.e., the $2 \Delta \theta_0$ value) can be used to determine the average perpendicular elastic strain. Because the thick GaN layer is fully relaxed, which is confirmed by the GaN(0002) peak position relative to the fully relaxed substrate $\text{Al}_2\text{O}_3(0006)$ peak (not shown), the position of the

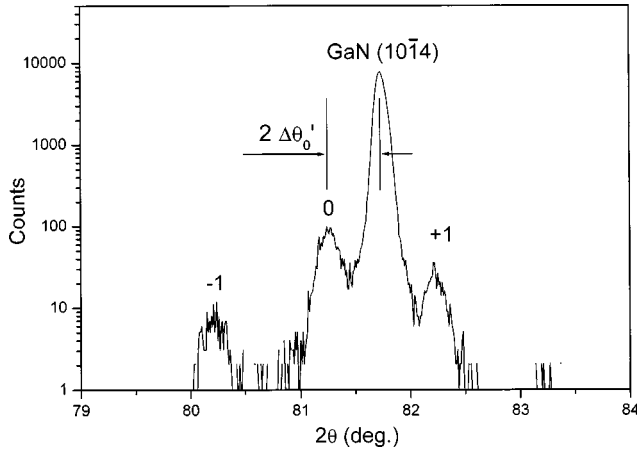


FIG. 6. X-ray $\theta-2\theta$ scan of the $(10\bar{1}4)$ diffraction from the sample in Fig. 1.

GaN(0002) peak can be taken as a reference to determine the correct position of zeroth peak $\theta_{\text{MQW}}(0002)$. In order to eliminate the influence of a possible misorientation angle between the thick GaN layer and the MQW, the measurement was repeated by rotating the sample 180° around its surface normal. Thus, two values $\Delta\theta_{0a}$ and $\Delta\theta_{0b}$, and $\Delta\theta_0 = (\Delta\theta_{0a} + \Delta\theta_{0b})/2$ were obtained. In this way, $\theta_{\text{MQW}}(0002) = \theta_{\text{GaN}}(0002) - (\Delta\theta_{0a} + \Delta\theta_{0b})/2 = 17.278^\circ - (0.10^\circ + 0.10^\circ)/2 = 17.178^\circ$ was determined. $\theta_{\text{GaN}}(0002) = 17.278^\circ$ is the bulk theoretical value of the GaN(0002) diffraction angle. $\Delta\theta_{0a} = \Delta\theta_{0b}$ implies that the epilayers in the MQW are parallel to the underlying thick GaN layer. Finally, the average lattice constant c of the epitaxial MQW, $\langle c_{\text{epi}} \rangle = \lambda / \sin \theta_{\text{MQW}}(0002) = 0.5214$ nm, is obtained. The zeroth peak is directly related to the average In composition $\langle x \rangle$ in the pair of InGaN/GaN layers,⁸ $\langle x \rangle$ being equal to $0.16 \times 2.7 / (2.7 + 7.7) = 0.042$. Hence, the average lattice constant $\langle c_b \rangle$ for bulk (i.e., unstrained) $\text{In}_{\langle x \rangle}\text{Ga}_{1-\langle x \rangle}\text{N}$ would be $0.5718 \times 0.042 + 0.5185 \times 0.958 = 0.5207$ nm, using Vegard's law and the lattice constants of InN and GaN.¹² Consequently, the average perpendicular elastic strain, including the estimated error, is $\langle e^\perp \rangle = (\langle c_{\text{epi}} \rangle - \langle c_b \rangle) / \langle c_b \rangle = 0.13\% \pm 0.02\%$.

F. Calculation of the average parallel elastic strain

In order to determine the average parallel elastic strain, an x-ray $\theta-2\theta$ scan from the $(10\bar{1}4)$ diffraction was performed (Fig. 6). Similar to the procedure for determining the $\theta_{\text{MQW}}(0002)$ from Fig. 1, the $\theta_{\text{MQW}}(10\bar{1}4)$ of

the $(10\bar{1}4)$ diffraction from the MQW is determined to be $\theta_{\text{GaN}}(10\bar{1}4) - (\Delta\theta'_{0a} + \Delta\theta'_{0b})/2 = 41.011^\circ - (0.25^\circ + 0.25^\circ)/2 = 40.761^\circ$. $\theta_{\text{GaN}}(10\bar{1}4) = 41.011^\circ$ is the theoretical bulk value of the GaN($10\bar{1}4$) diffraction angle. Subsequently, the average d spacing of the $(10\bar{1}4)$ plane of the MQWs is calculated to be 0.11793 nm. According to the d -spacing formula for a hexagonal crystal¹³ and the $\langle c_{\text{epi}} \rangle$ value determined from the (0002) diffraction, we experimentally obtained $\langle a_{\text{epi}} \rangle = 0.3196$ nm, $\langle a_{\text{epi}} \rangle$ being the average lattice constant a of the epitaxial MQW. From this value, an average parallel elastic strain and an estimated error $\langle e^\parallel \rangle = (\langle a_{\text{epi}} \rangle - \langle a_b \rangle) / \langle a_b \rangle = -0.25\% \pm 0.08\%$ are calculated, using the average lattice constant $\langle a_b \rangle = 0.3204$ nm for bulk $\text{In}_{\langle x \rangle}\text{Ga}_{1-\langle x \rangle}\text{N}$.

IV. CONCLUSIONS

Combining XRD, TEM, and RBS/channeling analyses, we have characterized the structure of an InGaN/GaN MQW and reliably determined the In content in the InGaN layer, which is important to determine the strain of the MQW. In this way, the average parallel elastic strain $\langle e^\parallel \rangle = -0.25\%$ and the average perpendicular elastic strain $\langle e^\perp \rangle = +0.13\%$ of the MQW are determined for a $[2.7 \text{ nm In}_{0.16}\text{Ga}_{0.84}\text{N}/7.7 \text{ nm GaN}]_{5x}$ MQW. Table I lists the average elastic strain of MQWs deduced from the literature and the results from this work. Table I shows that, on average, the MQW is under compressive strain in the parallel direction (i.e., $\langle e^\parallel \rangle$ is negative) and under tensile strain in the perpendicular direction (i.e., $\langle e^\perp \rangle$ is positive), as expected considering the sign of the lattice mismatch.¹⁴ By using the elastic constants c_{13} and c_{33} of GaN and InN used in Ref. 1, the average elastic constants $\langle c_{13} \rangle = 102.5$ and $\langle c_{33} \rangle = 397.4$ can be calculated using Vegard's law. Owing to $e^\perp/e^\parallel = -2c_{13}/c_{33}$,² $\langle e^\perp \rangle / \langle e^\parallel \rangle = -2\langle c_{13} \rangle / \langle c_{33} \rangle = -0.52$ can be deduced from the elastic constants. This is in excellent agreement with our experimental result $\langle e^\perp \rangle / \langle e^\parallel \rangle = +0.13\% / -0.25\% = -0.52$. We note that the strain values reported here are smaller than those deduced from literature. This was expected because of the lower average In composition in our sample.

ACKNOWLEDGMENTS

The authors are grateful to Xinhe Zheng for the simulation of the XRD data. Part of the experiments was carried out at the BSRF. This work has been performed within the framework of IUAP V-1 and was supported by the Key

TABLE I. Average elastic strain of MQWs deduced from literature and the results of this work.

Structure of MQW	Average In or Al composition $\langle x \rangle$	$\langle e^\perp \rangle$ (%)	$\langle e^\parallel \rangle$ (%)	Reference No.
7.6 nm $\text{In}_{0.17}\text{Ga}_{0.83}\text{N}/10.4$ nm GaN	0.072	0.40 ^a		8
5 nm $\text{Al}_{0.2}\text{Ga}_{0.8}\text{N}/5$ nm GaN	0.10	0.40 ^b	-0.85 ^b	9
2.7 nm $\text{In}_{0.16}\text{Ga}_{0.84}\text{N}/7.7$ nm GaN	0.042	0.13	-0.25	This work

^aEstimated from Fig. 1 of Ref. 8.

^bValues derived from the reported $\langle a_{\text{epi}} \rangle$ and $\langle c_{\text{epi}} \rangle$ data.

Laboratory of Heavy Ion Physics, Ministry of Education, China, by the National 863 High Technique Program of China under Grant No. 2001AA313060, by the National Natural Science Foundation of China under Grant No. 10375004, and by the Bilateral Cooperation between China and Flanders (BIL 99-07 and BIL 02-02). One of the authors (B. V. D.) is grateful to the Fund for Scientific Research-Flanders (FWO-Vlaanderen), Belgium.

- ¹S. Pereira, M. R. Correia, E. Pereira, K. P. O'Donnell, E. Alves, A. D. Sequeira, and N. Franco, *Appl. Phys. Lett.* **79**, 1432 (2001).
²S. Srinivasan, R. Liu, F. Bertram, F. A. Ponce, S. Tanaka, H. Omiya, and Y. Nakagawa, *Phys. Status Solidi B* **228**, 41 (2001).
³F. Scholz, J. Off, A. Kniest, L. Görgens, and O. Ambacher, *Mater. Sci. Eng., B* **59**, 268 (1999).
⁴M. Schuster, P. O. Gravis, B. Jobst, W. Hösler, R. Averbeck, H. Riechert, A. Iberl, and R. Stömmmer, *J. Phys. D* **32**, A56 (1999).

- ⁵M. F. Wu, A. Vantomme, S. Hogg, H. Pattyn, G. Langouche, W. Van der Stricht, K. Jacobs, and I. Moerman, *Appl. Phys. Lett.* **74**, 365 (1999).
⁶T. C. Wen and W. I. Lee, *Jpn. J. Appl. Phys., Part 1* **40**, 5302 (2001).
⁷M. F. Wu, S. D. Yao, A. Vantomme, S. M. Hogg, G. Langouche, J. Li, and G. Y. Zhang, *J. Vac. Sci. Technol. B* **17**, 1502 (1999).
⁸D. J. Kim, Y. T. Moon, K. M. Song, and S. J. Park, *Jpn. J. Appl. Phys., Part 1* **40**, 3085 (2001).
⁹D. Korakakis, K. F. Ludwig, Jr., and T. D. Moustakas, *Appl. Phys. Lett.* **72**, 1004 (1998).
¹⁰B. M. Paine, *Mater. Res. Soc. Symp. Proc.* **69**, 39 (1986).
¹¹L. R. Doolittle, *Nucl. Instrum. Methods Phys. Res. B* **9**, 344 (1985).
¹²T. Kachi, K. Tomita, K. Itoh, and H. Tadano, *Appl. Phys. Lett.* **72**, 704 (1998).
¹³M. F. Wu, A. Vantomme, H. Pattyn, G. Langouche, Q. Q. Yang, and Q. M. Wang, *J. Appl. Phys.* **80**, 5713 (1996).
¹⁴M. F. Wu, S. D. Yao, A. Vantomme, S. Hogg, G. Langouche, W. Van der Stricht, K. Jacobs, I. Moerman, J. Li, and G. Y. Zhang, *Mater. Sci. Eng., B* **75**, 232 (2000).